Salt water injection monitoring with crosshole EM: A report of 1992 field activities at the UC Richmond Field Station

D. L. Alumbaugh
A. Becker
H. F. Morrison
K.H. Lee
Lawrence Berkeley Laboratory

and

M. J. Wilt
Lawrence Livermore National Laboratory

January 26, 1993

Introduction

Beginning in 1988, a series of salt water injection experiments were conducted at the University of California Richmond Field Station test site to evaluate the use of different geophysical methods for monitoring the injection process and for determining the geometry of the resulting plume. The first set of experiments involved surface-to-borehole resistivity measurements and were conducted in February of 1988 and 1989 (Bevc and Morrison , 1992). Approximately 25,000 gallons of 1.0 ohm-m salt water were pumped into a 3 m thick, 30 m deep, flat lying aquifer. Resistivity measurements were made both before and after injection with current electrodes above, in, and below the aquifer with the potential electrodes at surface spaced at 5m intervals along lines radiating outward from the injection well (INJ in Figure 1). These experiments were useful in determing the migration path of the salt water, but no inversion of the data was attempted to determine the geometry of the injected plume.

In the spring of 1991 crossborehole electromagnetic (EM) measurements were made by Lawrence Berkeley Laboratory and Lawrence Livermore Laboratory personnel to track a similar volume

of injected salt water. About 36,000 gallons of water were employed in this experiment and cross-borehole EM data were collected both before and after the injection. The test employed two observation boreholes EMNE and EMSW (Figure 1) which are approximately equidistant from well INJ. The EM data were collected at a frequency of 18,800 Hz using a nearly continuous transmitter tool spacing of 0.2 m from the surface to a depth of 85 m in the EMSW well. The receiver station spacing was 5 m starting at the surface and extending to a depth of 85 m. Significant findings from that field experiment are summarized below:

- The salt water slug provided a good imaging target. The maximum difference in magnetic field amplitudes between measurements made before and after injection was more than ten percent and was easily detectable with our system. The anomaly was evident in a large number of the EM measurements.

- Operating at a frequency of 18.8 KHz in a noisy industrial environment, our data profile repeatability was approximately 3.0 percent in amplitude and 1.5 degrees in phase. This measurement accuracy was considerably worse than was achieved during a crosshole EM survey in Devine, Texas (Wilt et al. 1991).

- We could decipher a clear EM field anomaly due to the salt water injection but we were not able to successfully fit the field data with any numerical modeling code. Attempts were made using a 2.5-D inversion code (Zhou, 1989), and with a 3-D "block" model in a layered host (Tripp, 1991 personal communication). These efforts were not successful primarily because the surrounding medium is not one-dimensional and the salt water body was neither a two-dimensional object, nor a tabular block. The salt water plume appeared to be an irregular three-dimensional zone of varying salt concentration that followed the existing high permeability network around the injection zone.

Although the 1991 experiment at the Richmond field station was a technical success our mission was incomplete because we did not obtain a crosshole EM data set that was suitable for conductivity imaging with existing codes. Our "proven" code uses an assumption of two-dimensional geometry with a cylindrical symmetry (Alumbaugh and Morrison, 1992). To make proper use of this code we needed to acquire a data set with appropriate geometry and this was the primary goal for the field experiment in 1992.

The 1992 Richmond Field Station Experiment

The 1992 salt water injection experiment at Richmond was considerably more ambitious in scope than the 1991 effort. The experiment included the drilling of three new wells, each to a depth of 70 m, as well as an expanded set of field measurements. Well INJ1 (Figure 1) is a new injection borehole located 5 m southwest of the present injector (INJ). It has a plastic well casing perforated in a gravel aquifer at a depth of 26-30 m. It was necessary to drill this well since we wished to use it for imaging as well as fluid injection. The older injection hole (INJ) is unsuitable for use in EM imaging as it is only 35 m deep and has three segments of steel screening or casing that were previously used as resistivity current electrodes (Bevc and Morrison,1991). The new observation wells (EMNW and EMSE) were drilled along a NW-SE diagonal crossing over the new injection well such that the observation wells form the corners of a polygon centered on the new injector (Figure 1). The crosshole EM measurements were made with the transmitter deployed in the center (and injection) borehole and the peripheral boreholes were traversed with the receiver tool. This arrangement assured a "first-order" cylindrical symmetry required by the imaging code.

The 1992 experiment proceeded in much the same manner as the previous experiments. That is, crosshole EM data were collected before the saline fluid was injected and after the injection was completed. After an initial system setup and debugging session, a baseline crosshole EM data set was collected in May, 1992. It consisted of four crosshole profiles with the transmitter in the central well (INJ1) and the receiver tool deployed in each of the four EM observation holes. Data were collected at a frequency of 18,500 Hz using a transmitter tool spacing of 0.5 m from the surface to a depth of 60 m for each receiver position. Receiver stations were spaced 5 m apart from 5 m to 55 m in each of the four observation holes. Next, a volume of water was pumped into a 100,000 gallon holding pond and mixed with salt until the water conductivity was raised to 1 S/m. The fluid was then injected into borehole INJ1 at a rate of 10 gallons per minute for about 4 days. The total injected volume was approximately 50,000 gallons which is approximately 50 percent greater than that used in the 1991 experiment. Assuming a porosity of 30 percent, the injected water would sweep a

cylindrical space 3 m high and 8 m in radius. We collected a second set of crosshole EM and induction logging data during a four week period in June following the injection.

After the June measurements were made, fluid was pumped out of well INJ1 until the water conductivity was restored to the background value it had before the experiment began (60mS/m). The total volume pumped out was 300,000 gallons, about 6 times the amount injected. The pumping began on July 6 at a rate of 20 gallons per minute and it lasted 12 days. Water levels in the wells open to the aquifer were monitored during this period to better understand the hydrology of the site. The water was pumped into a drain that flows into San Francisco Bay. Finally after a two-week period which allowed the water level to recover its original position we attempted to repeat the baseline EM measurements in the EMNE well. Unfortunately, due to instrument problems data quality was much poorer than in May and this data was not retained. In all, the experiment was conducted over a period of three months.

The overall system deployment was very similar to that described by Wilt et al. (1991), with the exception that an audio power amplifier (Crown model 610) was used for signal power amplification instead of the Zonge GGT-20 transmitter. The Crown amplifier has a high frequency limit in excess of 20,000 Hz, whereas the Zonge transmitter was limited to 8,000 Hz. This higher frequency capability is essential at Richmond because the boreholes are closely spaced and the background resistivity is relatively high (≈20 ohm-m). Other changes included the use of lightweight, portable winches, short segments of logging cable and the use of a special transmitter cable capable of carrying10 amps of current.

In general, we found that the data repeatability and reciprocity errors for the Richmond1992 experiment were two to three times worse than those at Devine, Texas (Wilt et al. 1991) and similar to those observed in the 1991 data set. We feel that the noise level is higher at Richmond because of the higher frequencies involved and closer physical proximity of the source and receiver instrument vans. Both of these factors allow for variable surficial coupling of the high level transmitter signal to the receiver. Although considerable time was spent before both the Devine and Richmond tests removing "ground-loops" from our system, additional errors (and ground loops) were evident in the Richmond data, primarily as the result of these more difficult operating conditions. Secondly,

because Richmond is located in an industrial area, external noise (from grounded power lines, BART etc.) is more of a problem and constitutes an unknown source of error.

Crosshole EM Profiles

Ten sets of cross-well data were collected with the transmitter in INJ1 and the receiver in each of the four surrounding EM wells. Four of these data sets were collected before injection and six after injection. In order to present all the data in any one cross-well set simultaneously, they were first normalized to a source strength of unit dipole moment. Then the amplitude and phase were plotted in a gray scale format as a function of transmitter and receiver position . Figures 2 and 3 show the EMNW data sets before and after injection, respectively. Plotting the data in this manner allows us to check for data continuity between profiles and also determine any changes that take place due to the injection.

Figures 2 and 3 clearly show the data both before and after injection to be smoothly varying both along each individual profile and in between the individual lines. Although the magnitudes of the changes are not spectacular, a decrease in amplitude and an increase in phase can be seen at a transmitter depth of approximately 30m when the post injection data is compared to the pre injection data. These changes are caused by the injection of salt water and are consistent with models run in the design phase of the experiment.

The effects of the injection become much more apparent if we calculate the secondary fields resulting from the introduction of the plume. This is a simple process involving the subtraction of the fields measured before the injection from those measured after injection. The resulting anomalies shown in Figure 4 clearly indicate large changes that are not readily apparent in the raw data. The fact that the anomalies are several times larger than the noise estimates suggests that the EMNW data are of sufficient quality to be used in various imaging schemes.

It was noticed both during the data collection as well as during the processing that the data quality appeared to decrease in a clockwise fashion from the EMNW well to the EMSW well. This can be displayed by calculating the secondary fields in the EMSW data resulting from the salt water injection. Although the pre-injection

and post-injection data (Figures 5 and 6) appear to be fairly consistent, the secondary fields (Figure 7) do not show the same character as those in the EMNW data or in the earlier numerical and scale model studies. This may be due in part to noisier data, but also could result from the plume moving away from INJ1 in a northerly direction as suggested by earlier experiments (Bevc and Morrison, 1990) rather than spreading symmetrically about the injection well. Comparing these results with those obtained in the EMNE and EMSE wells suggests that this may be the case as the EMNE data show a large anomaly resembling the one present in the EMNW data while the EMSE data show results similar to the EMSW measurements.

Interpretation of Data

One of the prime considerations of the Richmond '92 experiment was to produce a data set in which the geology, to a first order, exhibits a geometry suitable for our 2-D inversion routine. This routine assumes a cylindrical symmetry of the conductivity distribution about the transmitter borehole in an otherwise homogenous half space. It uses an iterative Born scheme to linearize the problem and regularized least squares to invert for the conductivity distribution (Alumbaugh and Morrison, 1992).

Because the Richmond geology consists of interbedded conductive shales and sands overlying a more resistive basement, the plume can't be interpreted as being injected into a homogenous half-space. Thus rather than inverting only for changes in conductivity resulting from the injection, the entire conductivity structure between the two wells was imaged both before and after injection and the results compared. The background conductivity used in the process was chosen by minimizing the magnitude of the secondary field.

Figure 8 shows the images obtained by inverting the pre- and post-injection data collected in the EMNW well. Though it does not indicate flat lying layers, the pre-injection image does show conductive overburden overlying a more resistive basement. The post-injection image clearly shows a high conductivity anomaly that corresponds to the injection zone. This strongly suggests that the salt water has migrated to the northwest which agrees very well with the results published by Bevc and Morrison (1991). Inversions

of the other data support this conclusion. Images of the EMNE data (Figure 9) indicate some migration to the northeast while the EMSW inversions (Figure 10) indicate almost no migration to the southwest. The direction of plume migration becomes even more apparent if we plot the change in conductivity between the before and after images as shown in Figure 11.

Notice that the inversions from EMSE have not been included here. This is due to the fact that the average misfits to these data was over 20% compared to 10% or less for data collected in the other three wells. This large misfit may be due to extreme 3D geology between the two wells, poor data quality, or a combination of both.

Conclusions

The 1992 Richmond field experiment showed that a salt water injection process can be monitored using cross well electromagnetics. Although the crosswell EM system worked fairly well there is definite room for improvement as there were significant drift problems and repeatability errors. However even with these problems the data is in most cases of sufficient quality not only to detect the presence of the body but also to allow for simple imaging schemes to be applied. Results from this imaging process correlate well with previous experiments which show the plume to be moving off to the northwest. Additional 3D modeling needs to be done both to verify this as well as to test the limits of the 2-D inversion code.

Acknowledgment

The field personnel consisted of Dave Alumbaugh, Maryla Deszcz-Pan, and H. W. Tseng of the University of California at Berkeley, and Mike Wilt from Lawrence Livermore National Lab. Technicians Jim Doherty and Don Lippert from Lawrence Berkeley Lab reworked the plumbing system for the salt water injection and extraction and provided technical support for the project. Peter Persof from LBL was in charge of the water level measurements made during the salt water extraction. This work was done under the sponsorship of the DOE (OBES and FOSSIL) programs. Principal funding for the field experiment was provided by an industrial research consortium that

included MOBIL, SCHLUMBERGER, SHELL, NORANDA, EXXON, NMC, BRITISH PETROLEUM, TEXACO and AMOCO.

References

Alumbaugh D.L., and Morrison, H.F., 1992, Tomographic Imaging of Cross well EM Data Extended abstracts from the Society of Exploration Geophysicists 1992 annual meeting, New Orleans, Louisiana.

Bevc, D. and Morrison, H.F, 1991, Borehole-to-surface electrical conductivity monitoring of a salt water Injection experiment. Geophysics **56** no. 6 p 769-777.

Pouch, G.W., 1987, Hydrogeological Site Assessment of the Engineering Geoscience Well Field at the Richmond Field Station, Contra Costa County, California. Unpublished MS Thesis, Department of Material Sciences and Mineral Engineering, University of California, Berkeley.

Waxman, M.H. and E.C. Thomas, 1974, Electrical conductivities in shaly sands-I the relation between hydrocarbon saturation and resistivity index. Journal of Petroleum Technology 213-215; transactions AIME, 257.

Wilt, M.J., Morrison, H.F., Becker, A., and Lee K.H., 1991, Cross-borehole and surface-to-borehole electromagnetic induction for reservoir characterization. DOE report DOE/BC/91002253.

Zhou, Q., 1989. Audio-frequency Electromagnetic Tomography for Reservoir Evaluation. Ph D Thesis Department of Engineering Geosciences, University of California, Berkeley.

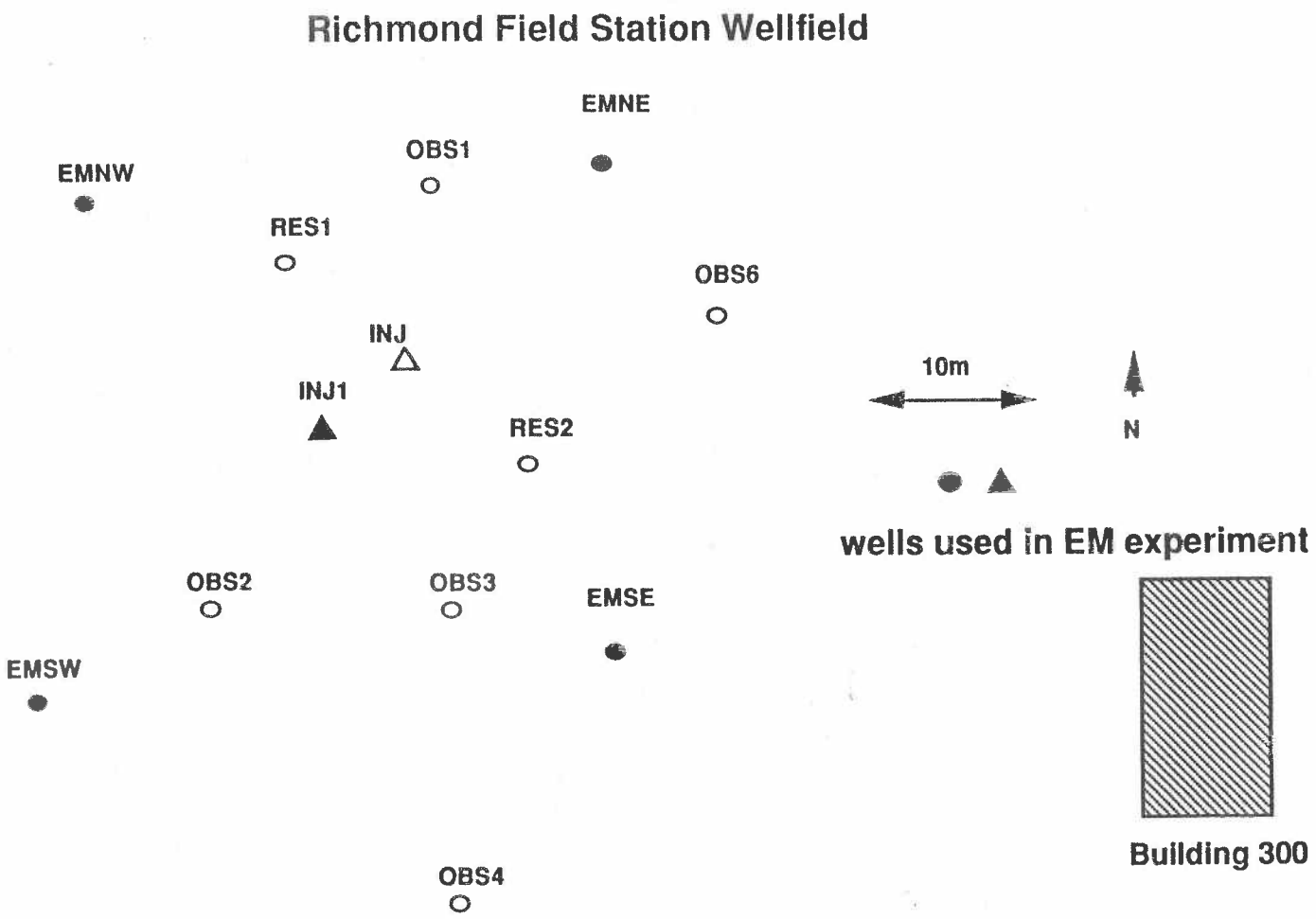

Figure 1. Location map for the building 300 w300 well field at the Richmond Field Station.

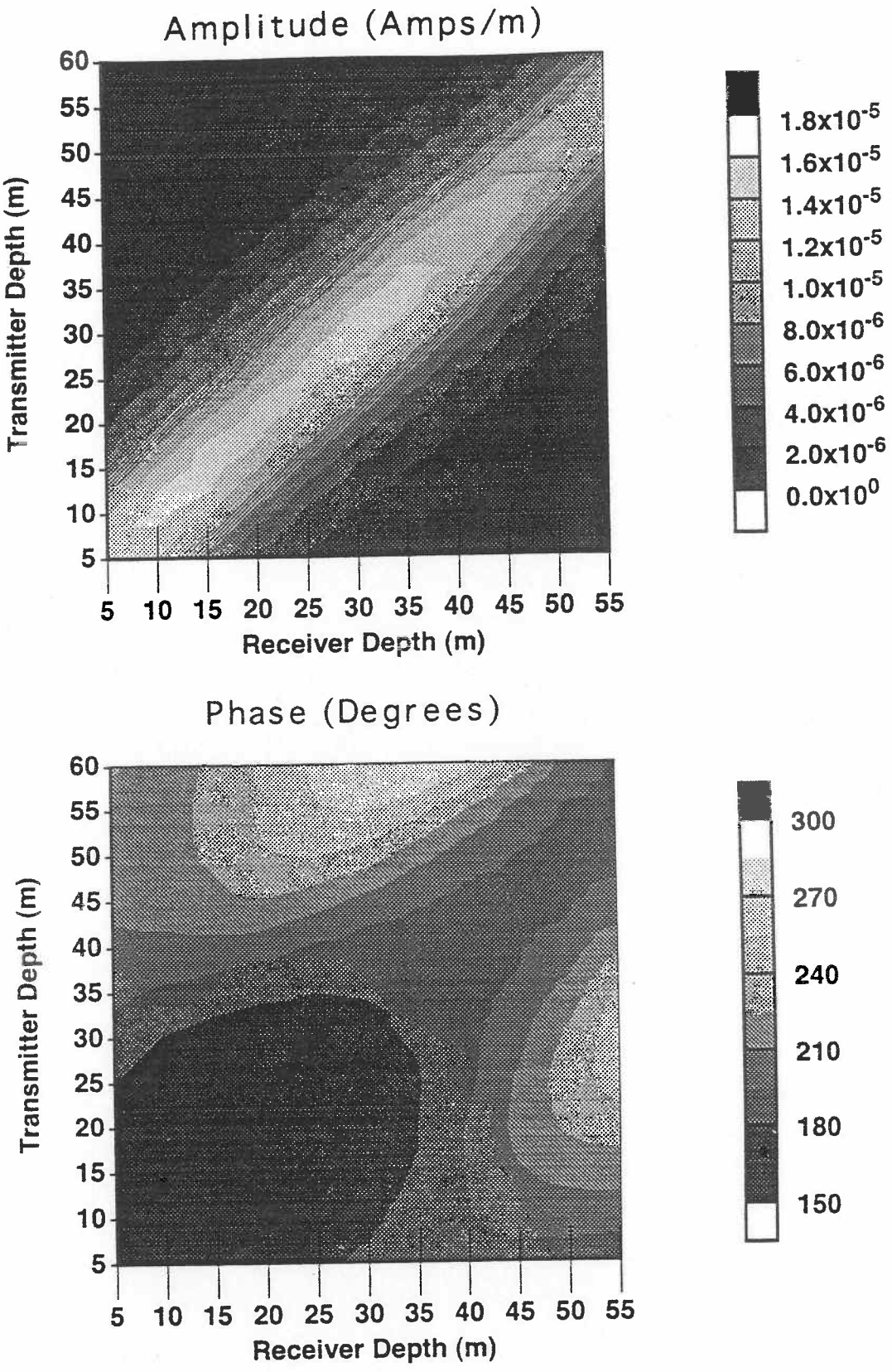

Figure 2 - EMNW data amplitude and phase prior to injection. Each line on the receiver axis represents an individual profile of continuous data in transmitter depth.

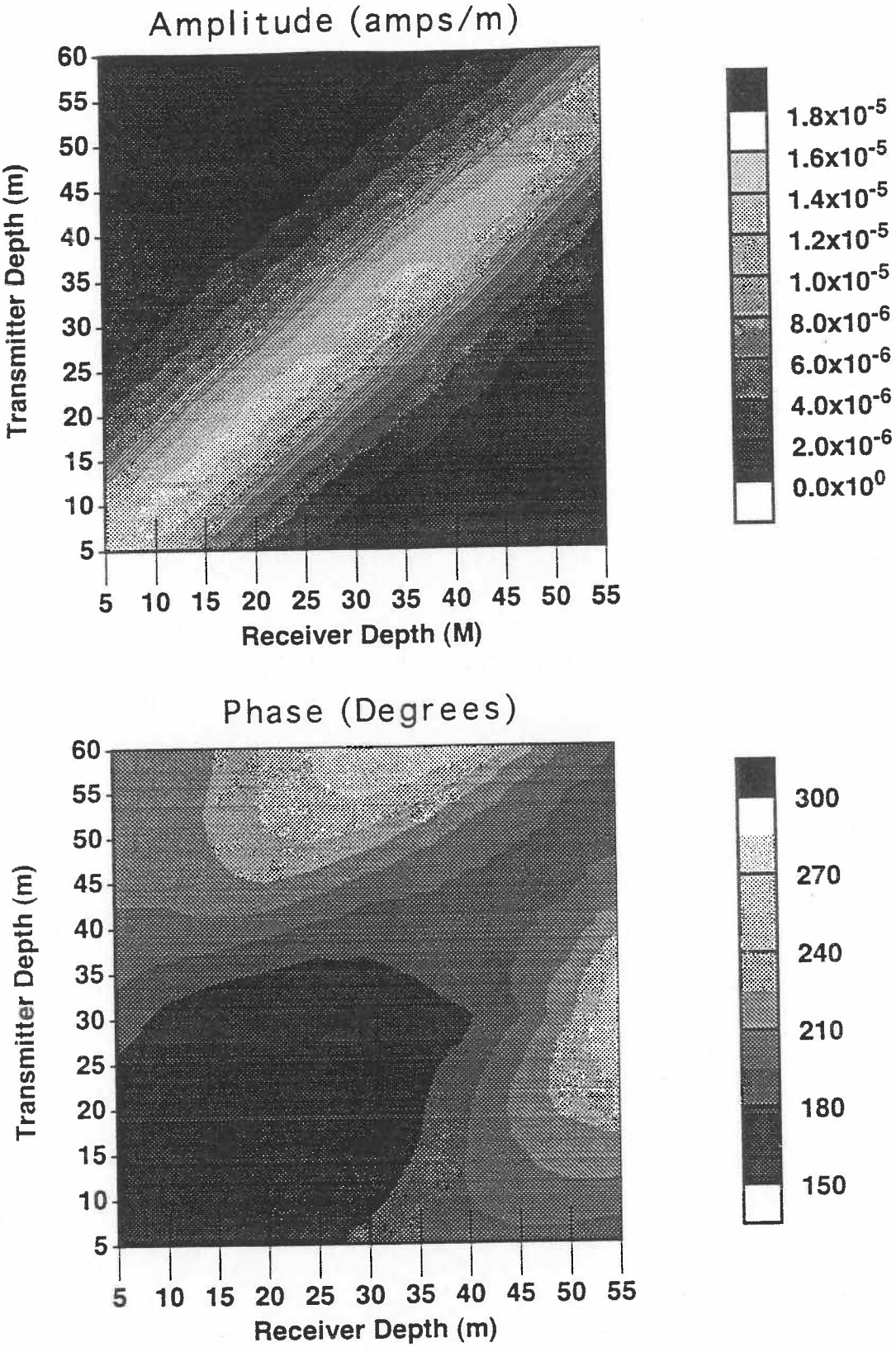

Figure 3- EMNW data amplitude and phase after injection. Each line on the receiver axis represents an individual profile of continuous data in transmitter depth.

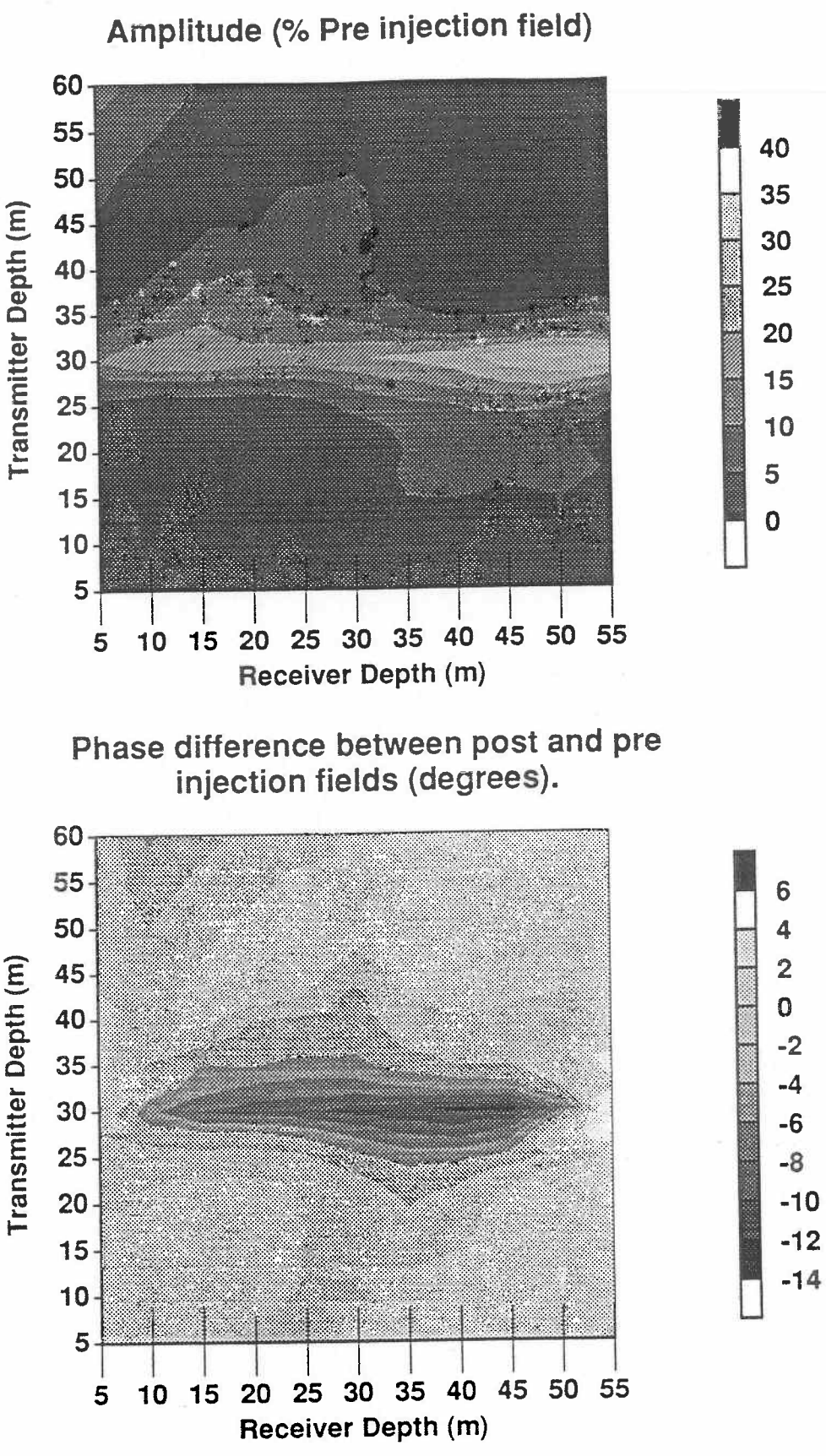

Figure 4 - EMNW secondary fields calculated by subtracting the preinjection data from the postinjection data. Each line on the receiver axis represents an indivdual profile of continuous data in transmitter depth.

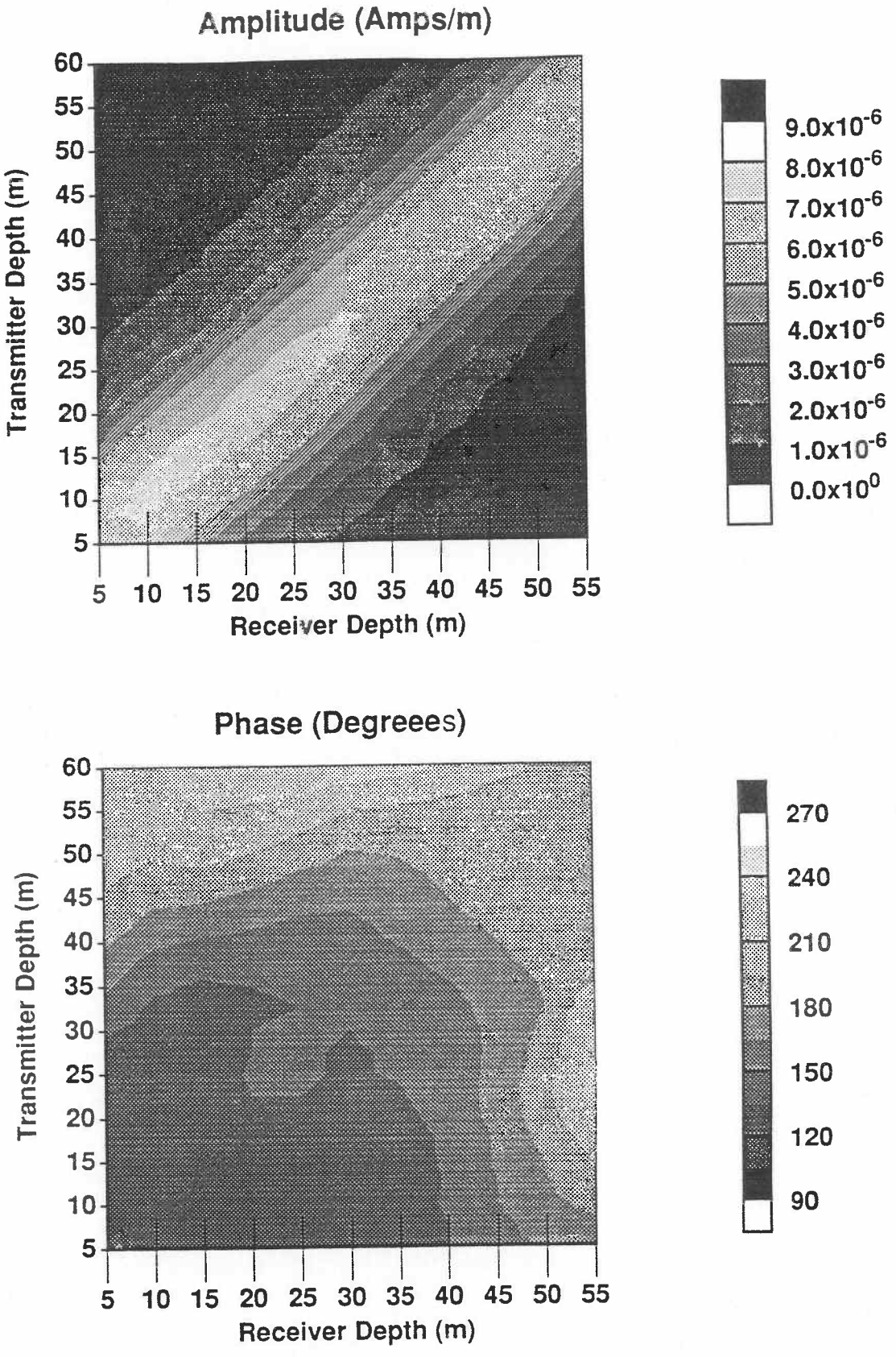

Figure 5 - EMSW data amplitude and phase prior to injection. Each line on the receiver axis represents an individual profile of continuous data in transmitter depth.

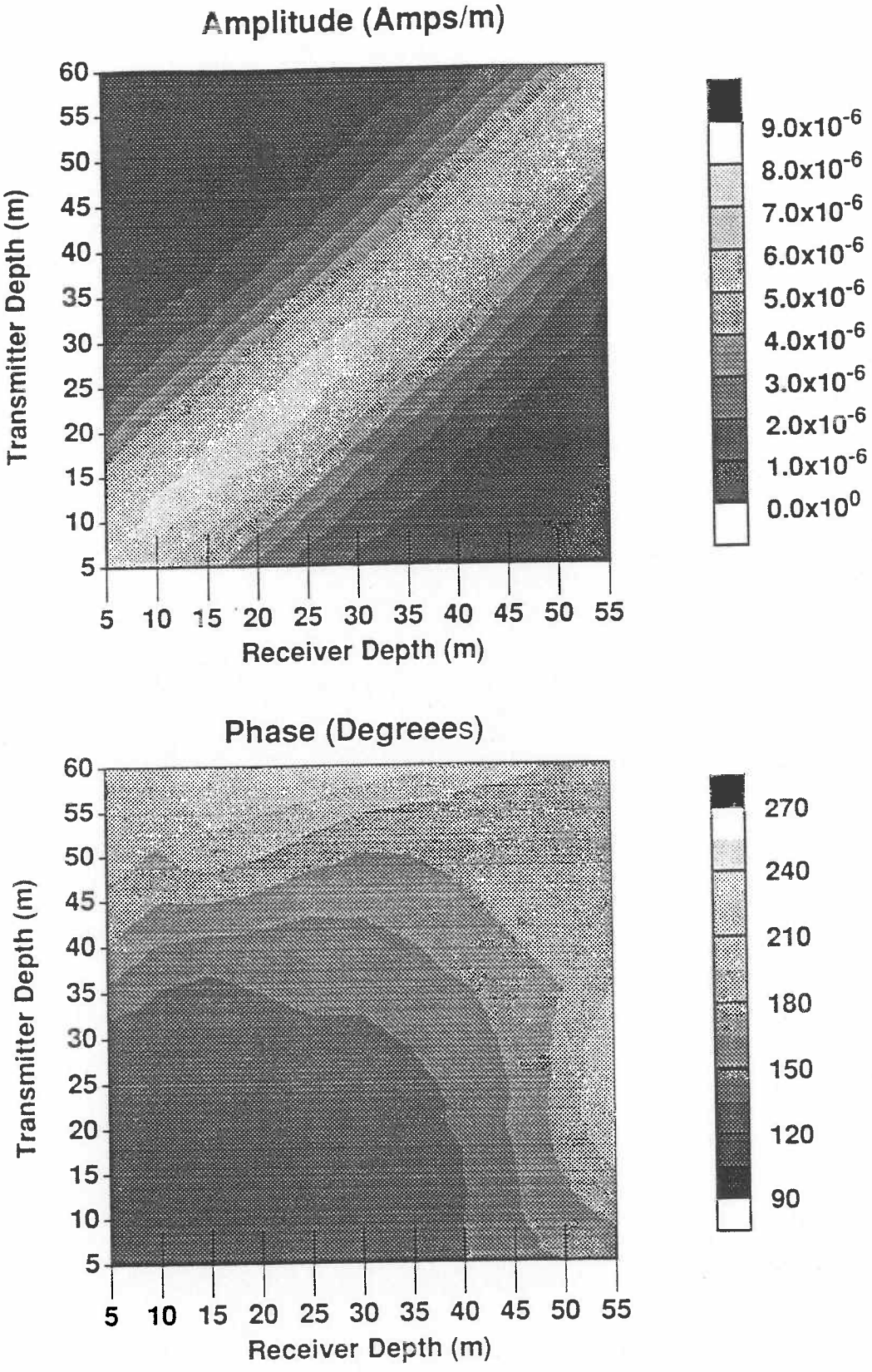

Figure 6 - EMSW data amplitude and phase after injection. Each line on the receiver axis represents an individual profile of continuous data in transmitter depth.

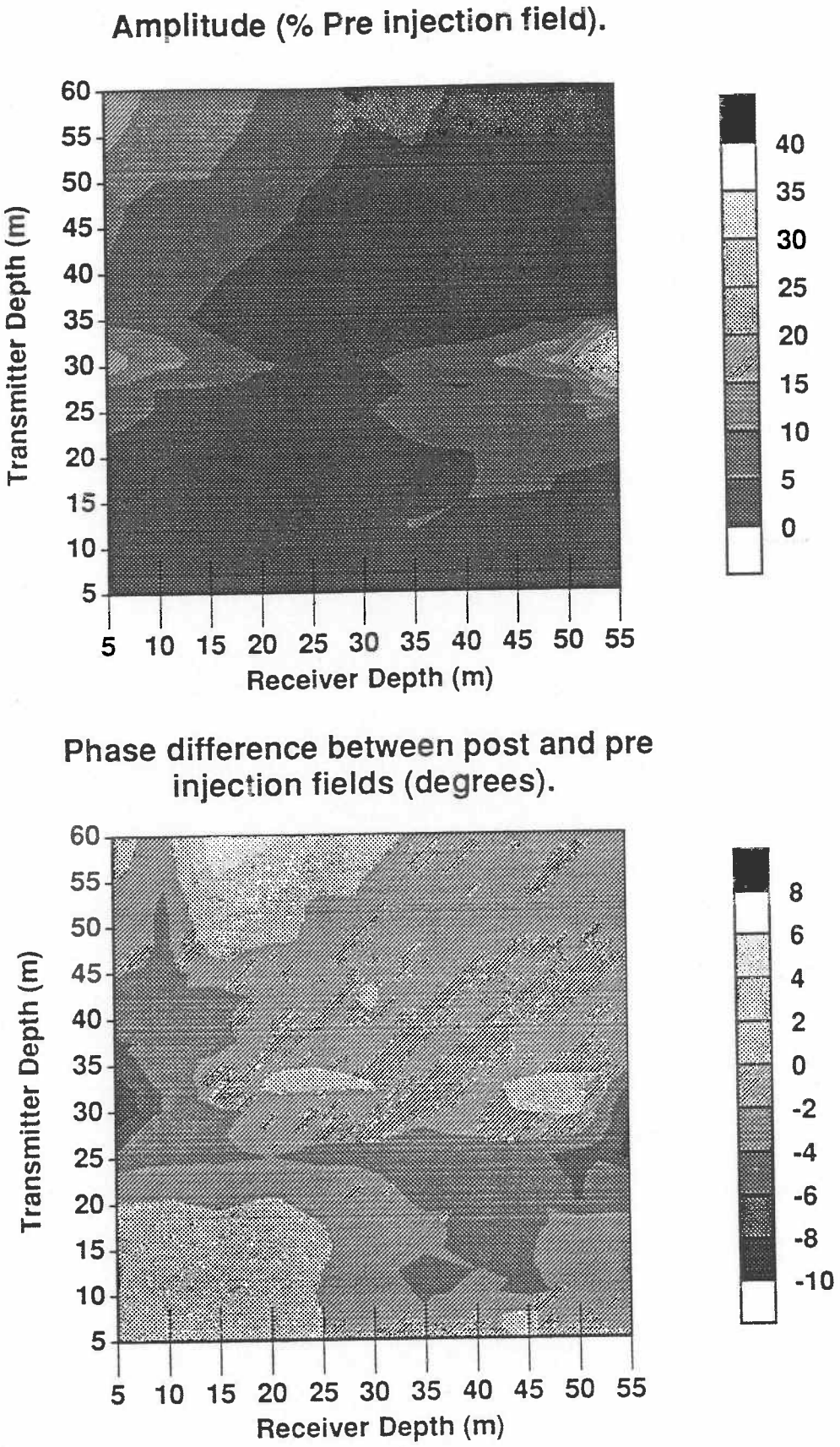

Figure 7 - EMSW secondary fields calculated by subtracting the preinjection data from the postinjection data. Each line on the receiver axis represents an individual profile of continuous data in transmitter depth.

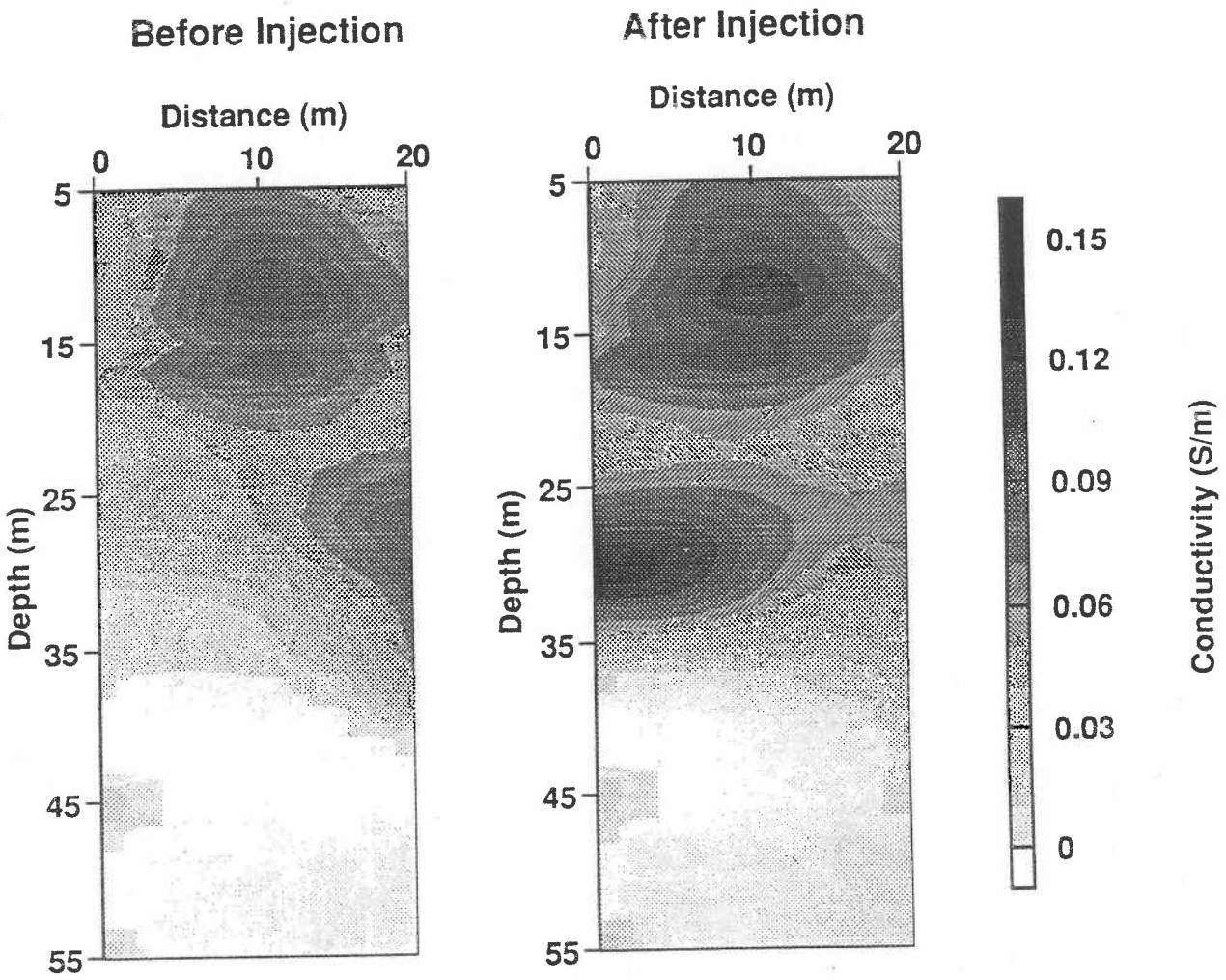

Figure 8 - Iterative Born inversion of EMNW data.

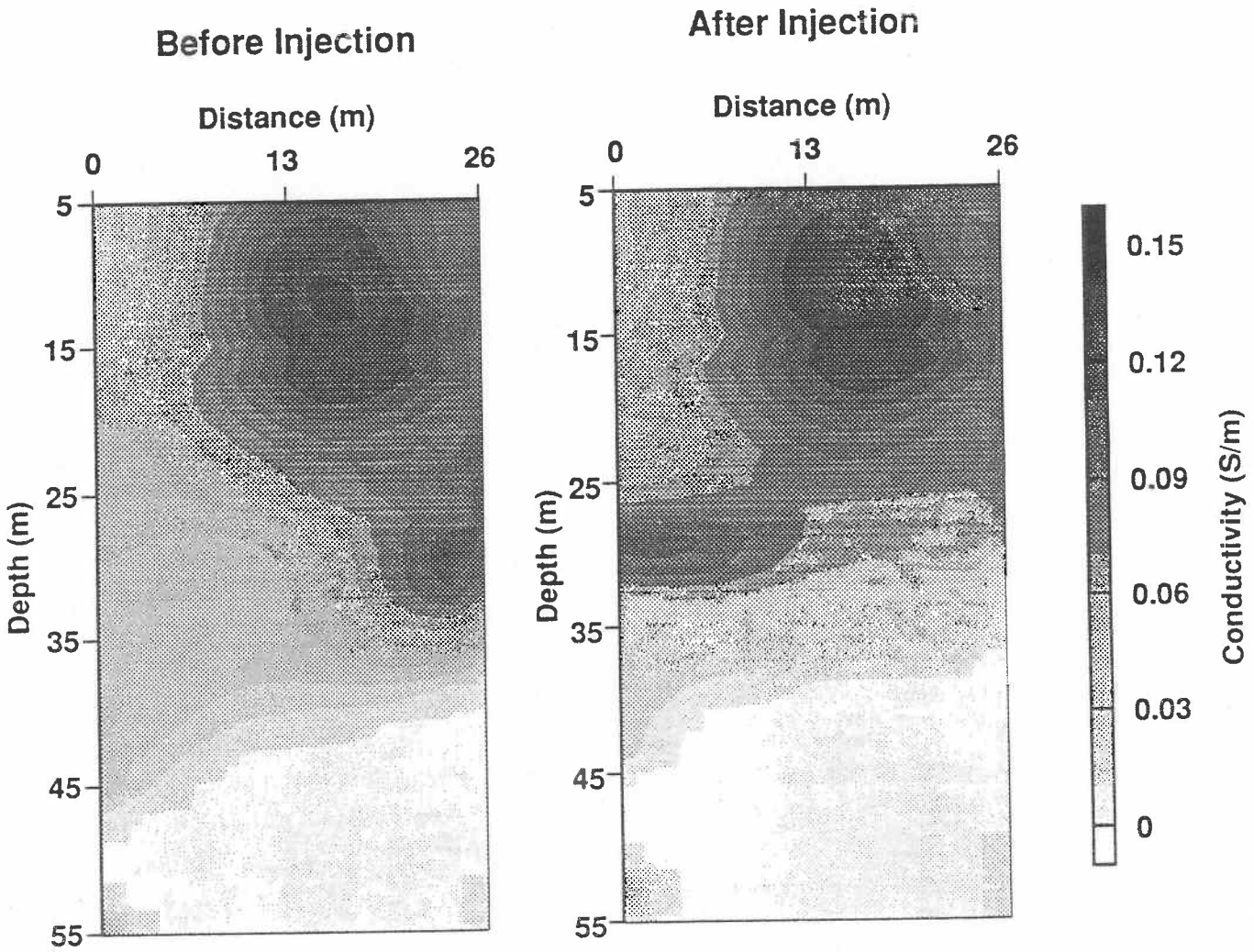

Figure 9 - Iterative Born inversion of EMNE data.

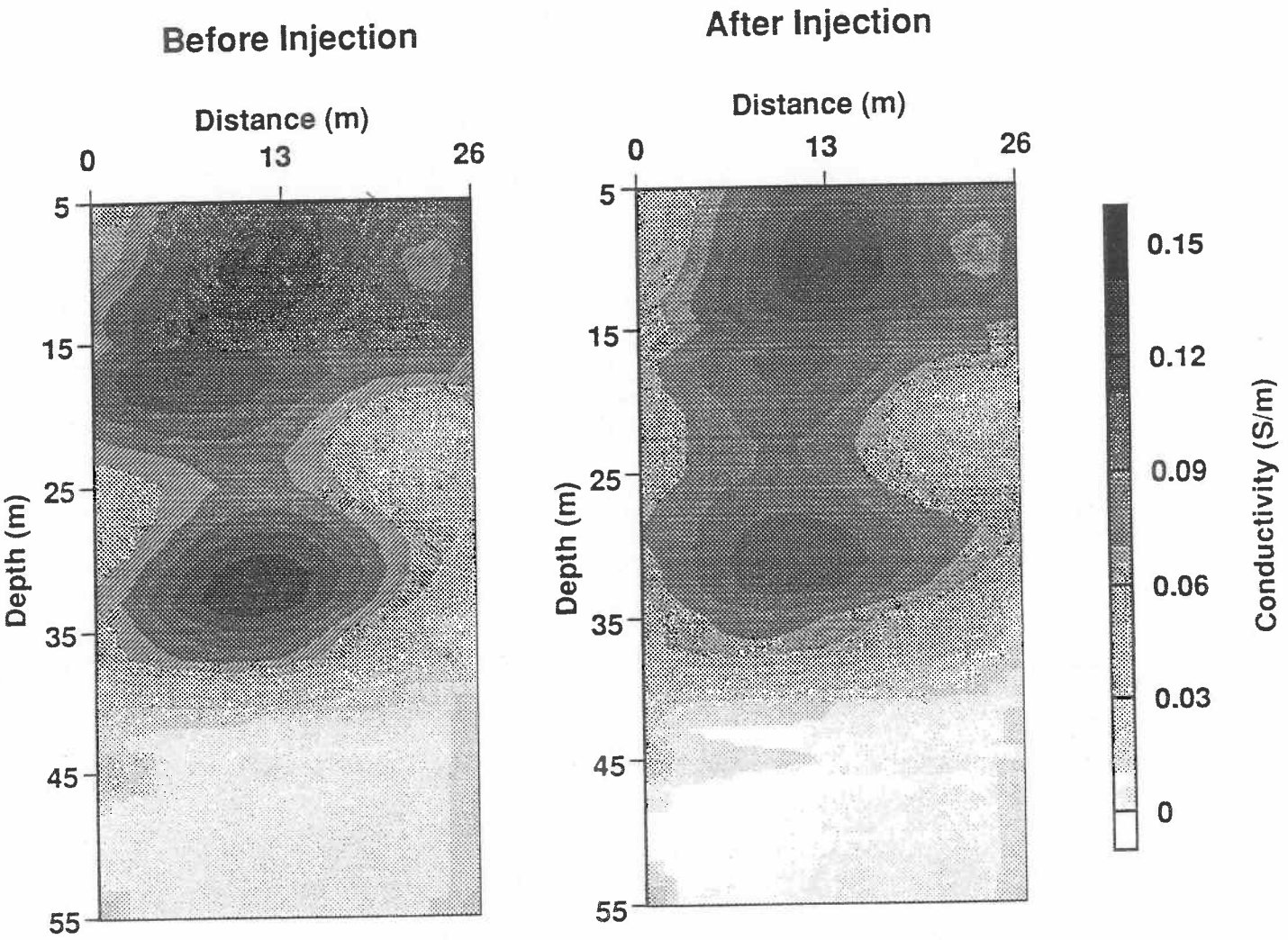

Figure 10- Iterative Born inversion of EMSW data.

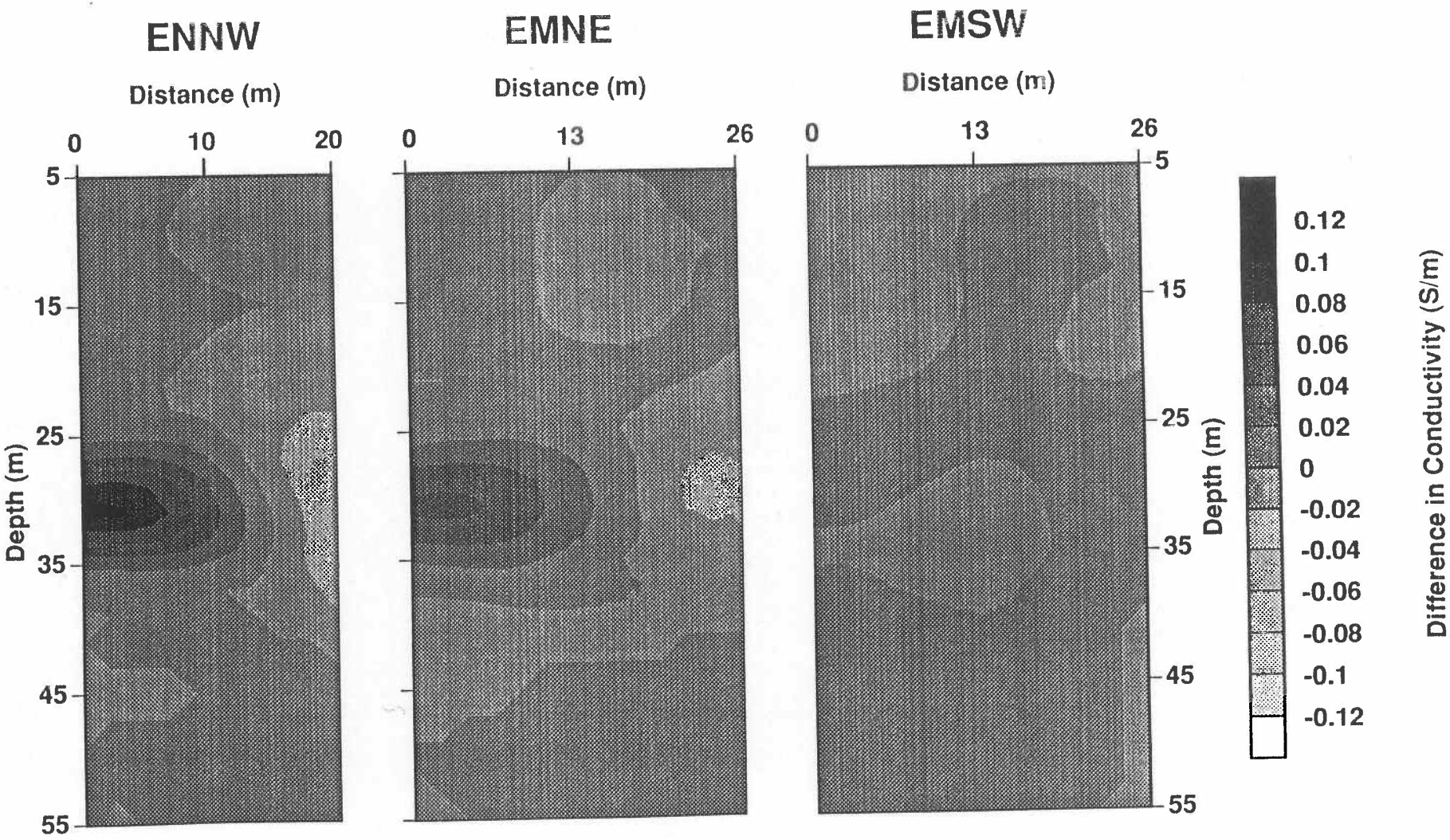

Figure 11 - Difference in conductivity between the postinjection and preinjection images in Figures 8, 9 and 10.